EURODYN 2020
XI International Conference on Structural Dynamics
M. Papadrakakis, M. Fragiadakis, C. Papadimitriou (eds.)
Athens, Greece, 22–24 June 2020

CONTRIBUTION OF SEISMIC NOISE RECORDINGS TO THE NON-STRUCTURAL VULNERABILITY ASSESSMENT

Konstantinos G. Megalooikonomou[1]

[1] GFZ German Research Centre for Geosciences, Helmholtz Centre Potsdam, Section 2.6: Seismic Hazard and Risk Dynamics, Helmholtzstraße 7, 14467 Potsdam, Brandenburg, Germany
e-mail: kmegal@gfz-potsdam.de

Keywords: ambient vibrations, induced seismicity, non-structural components, masonry

Abstract. *Since the 1990s, the recordings of ambient vibrations in structures have gained interest in the civil engineering community due to technological improvements of portable sensors, allowing the recordings of small amplitude vibrations, and the possibility of processing a large amount of data even in real time. Many applications, based on the analysis of seismic noise, exist in the literature for checking the serviceability limit state of existing construction in the case of earthquakes. These applications can be extended to the case of occurrence of induced and triggered seismicity and its potential impact on the built environment. The latter impact has heightened both public concern and regulatory scrutiny, emphasizing the need for an integrated risk management framework. Considering the case of induced seismicity, the vulnerability assessment requires the expected damage to refer to non-structural components. In this study, some historical masonry buildings located in Alsace France are considered and the dynamic characteristics of these structures were estimated by the analysis of seismic noise recordings by sensors installed at each floor of the buildings under study. The estimated dynamic properties for small amplitude vibrations of these historical structures were used to derive simplified vulnerability models. Moreover, the Eurocode 8 defines the interstory drift limit of a building for non-structural damage, by looking at its displacement-sensitive non-structural components at the serviceability limit state. Therefore, by adopting these limits and the developed simplified vulnerability models, new fragility curves for typical historical masonry building types dominant in the region under study are proposed. The fragility curves have been calculated using incremental dynamic analysis for the seismic demands generally imposed upon linear and slightly non-linear models of single and multiple degrees of freedom, which is the case for the effects of induced seismicity. These results will prove useful for both local end-users and industrial stakeholders, with a clear perspective for a better understanding of the risk related to induced and triggered seismicity and its sound management.*

1 INTRODUCTION

Since the 1990s, the recordings of ambient vibrations in structures have gained interest in the civil engineering community due to technological improvements of portable sensors, allowing the recordings of small amplitude vibrations, and the possibility of processing a large amount of data even in real time. Many applications, based on the analysis of seismic noise, exist in the literature for checking the serviceability limit state of existing construction in the case of earthquakes. These applications can be extended to the case of occurrence of induced and triggered seismicity and its potential impact on the built environment. The latter impact has heightened both public concern and regulatory scrutiny, emphasizing the need for an integrated risk management framework. Considering the case of induced seismicity, the vulnerability assessment requires the expected damage to refer to non-structural components.

The ultimate goal of seismic design of a structure is to prevent structural collapse and human losses in case of an earthquake event. Over time, advances in earthquake engineering have led to a wide range of methodologies for earthquake resistant structural design. As a result, structures built with current methods are generally able to resist expected seismic activity and preserve their structural integrity. However, although a building remains structurally sound, it can be rendered unusable due to damage to its non-structural components. Additionally, the majority of the value of some specific buildings lies in their non-structural components. For instance, it has been shown that non-structural components account for 82%, 87% and 92% of building costs for offices, hotels and hospital buildings, respectively [1]. Therefore, building owners may still be burdened with high expenses due to the need to repair and replace non-structural components, despite applying the current seismic design standards.

The Eurocode 8 (Cl.4.4.3.2) [2] defines the maximum interstory drift (IDR) limit of a building for non-structural damage of its displacement-sensitive non-structural components for the serviceability limit state. The latter relates to structural performance for normal service conditions, under which the function of a building, its appearance, maintainability, durability and comfort for its occupants must be preserved. In that case, the IDR obtained from elastic analyses should be limited to the following values, set as a function of the non-structural typology/detailing and represented by θ_{ns}, which is the limiting story drift ratio, equal to the relative inter-story displacement divided by the story height:

- for buildings having non-structural components fixed in a way so as not to interfere with structural deformations: $\theta_{ns} \leq 1.0\%$;
- for buildings having ductile non-structural components: $\theta_{ns} \leq 0.75\%$;
- for buildings having non-structural components, realized with brittle materials, attached to the structure: $\theta_{ns} \leq 0.5\%$.

It is not clear from the above definitions in Eurocode 8 how ductile non-structural components are distinguished from the other mentioned types. In addition, a minimum required ductility capacity is not provided in these guidelines. Moreover, the drift limit of 1.0% for non-structural components fixed in a way not to interfere with structural deformations appears to be very high for masonry structures and there are not clear indications of how it is set to this value also for this case. However, the above criteria provide a test-bed for drift sensitive non-structural damage to be considered as damage thresholds in the analytical definition of fragility curves.

In this paper the focus will be on the rapid and efficient modeling of an urban area from the vulnerability point of view (considering only the possible damage to non-structural components), which is the key component for the efficient and reliable implementation of risk monitoring applications.

2 CASE STUDIES

In this study, some historical masonry buildings located in Alsace France are considered and the dynamic characteristics of these structures were estimated by the analysis of seismic noise recordings by sensors installed at each floor of the buildings under study (Fig. 1).

In the considered test site, the analysis of the collected exposure information indicates that traditional or historical masonry structures occur in large numbers near in the mostly rural areas close to the geothermal platforms in Alsace region in France [3]. Two general classes of structures, namely unreinforced masonry (URM) and timber-framed masonry (TFM) buildings have been considered, and the simple performance assessment models ([4], [5]) have been adopted in order to carry out a preliminary vulnerability assessment for these classes of structures. The objective is to rapidly identify buildings and their non-structural components that are at greater risk in the event of an induced earthquake, and to model their non-structural fragility.

The vulnerability modelling focused on buildings constructed of masonry, which may be more susceptible to the range of ground motion expected in the event of induced seismicity in the area. The measurements have been carried out using the MPwise (Multi-Parameter Wireless Sensing System) smart device [6], which has been designed to carry out rapid measurement activities by exploiting the computing and advanced networking capacities embedded in individual units. Based on measurements of environmental seismic noise, the fundamental frequency of vibration of the inspected buildings has been estimated and used to calibrate the respective fragility curves.

In collaboration with GFZ and ES-Géothermie a three-day acquisition campaign was organized which involved the installation of four sets of sensors in private houses located in villages located around the Soultz and Rittershoffen geothermal sites. The fundamental period of these structures was verified by analyzing the ambient noise measured using the MPwise sensors [6], with one sensor installed outside of the buildings, and the three others installed on each floor of the houses (basement, ground floor and first floor). The sensors were installed to record the ambient noise and to draw a vulnerability mode that allows the issuing of damage forecasts (Table 1, [7]). Finally, the main geometry required as input for the simplified vulnerability models was taken through field inspection of these buildings.

No	Building Type	Building Latitude	Building Longitude	Fundamental ESDOF Model Period (s)	Fundamental Frequency Sensor (Hz)
1	URM	48.964946	7.881095	0.17	5.5
2	URM	48.902075	7.874917	0.37	2.7
3	URM	48.905270	7.950266	0.11	9
4	TFM	48.914307	7.882233	0.15	6.7
5	URM	48.932865	7.874377	0.32	3.1

Table 1: Real URM and TFM buildings located near the geothermal platforms in Alsace region in France [7].

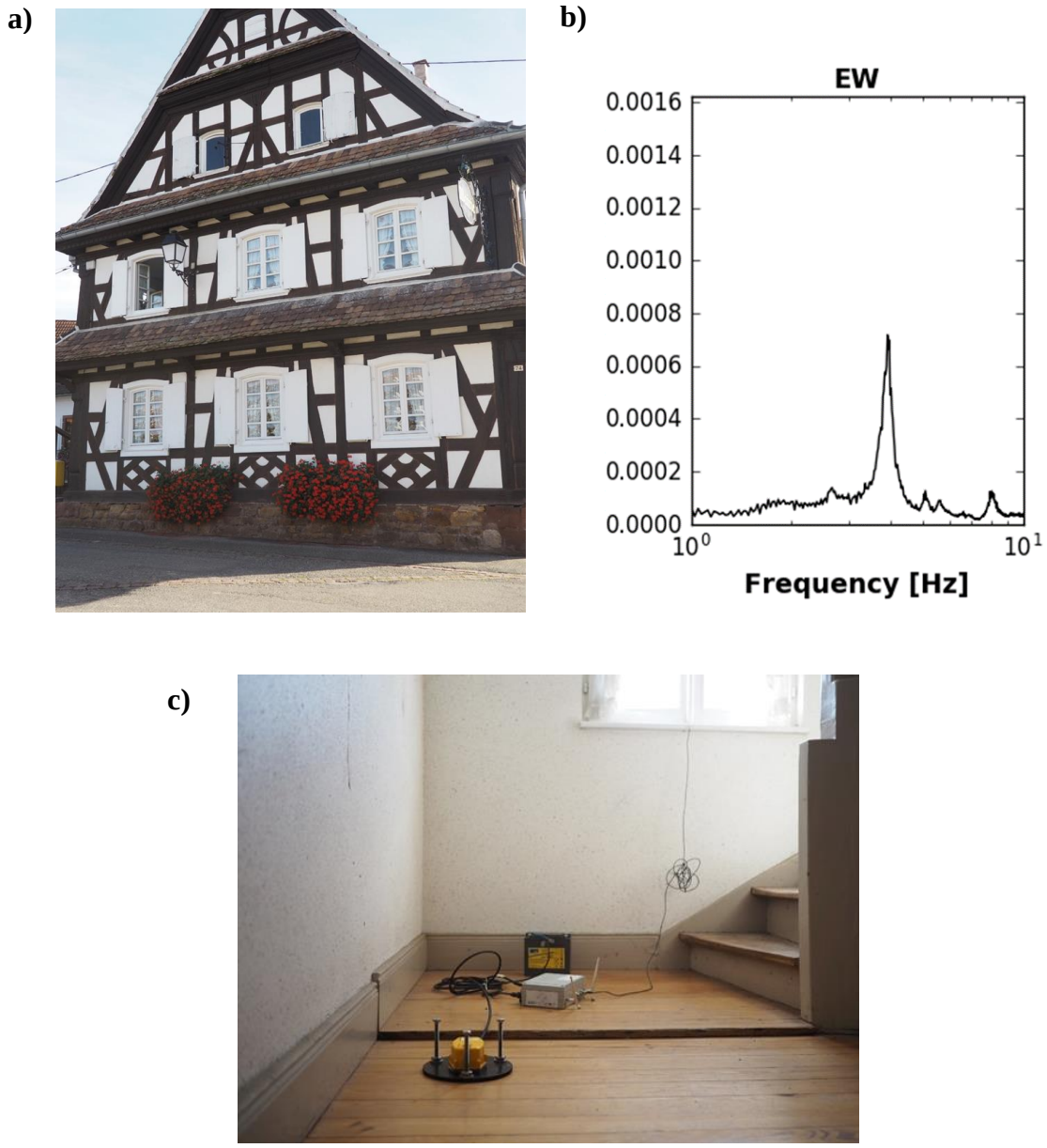

Figure 1: a) Example of timber-framed masonry building b) Measurements of the fundamental frequency of vibration estimated from the spectral analysis of environmental seismic noise. c) Installation of MPwise floor sensor

3 VALIDATION OF THE NUMERICAL MODEL

The estimated dynamic properties for small amplitude vibrations of these historical structures were used to derive simplified vulnerability models.

While steel or concrete frames are mostly lumped systems with stiff diaphragms, URM buildings have distributed mass and stiffness commonly in combination with flexible diaphragms. This fact obstructs the adoption of the established methodologies to URM buildings. Specifically, the fundamental mode shape of the latter buildings involves a low percentage of the total mass of the building below the 75% limit required for the good performance of ESDOF-based methods. In order to solve this issue, the simplified procedure of Vamvatsikos et al. (2015) [4] was adopted. In their procedure the dynamic URM building response is repre-

sented. Global response indices are transformed to local deformation measures in closed-form seismic assessment solution both for demand and supply in the critical structural locations. The solution involves the definition of the fundamental vibration mode, approximated by 3D shape function consistent with the building's boundary conditions. Strength and deformation indices are adopted for the evaluation of the acceptance criteria. Typical local failures are estimated through a local shape of deformation while the model captures the global dynamic characteristics. The adopted method allows the automation of the necessary calculations through closed-form expressions. The application of the methodology presented in this work to produce the analytical fragility curves for URM buildings is demonstrated here (Table 2) on a box-shaped unreinforced masonry structure of the townhall of Keffenach (URM building No.1 in Table 1) in Alsace region in France near the geothermal platforms of this region (Soultz-sous-Forêts and Rittershoffen).

Longitudinal wall length	9.14 m
Transverse wall length	12.04 m
Roof height	3.5 m
Wall thickness	0.25 m
Shear Modulus	930 MPa
Shear Strength	0.93 MPa
Wall mass	75.57 tn
Story mass	2.1 tn
Roof mass	3.27 tn
Total mass	80.94 tb
Horizontal "gravity" load	226.85 kN/m
Wall total area	10.59 m^2
Wall box moment of inertia	157.64 m^4
Resistance of wall plan	33.58 m^3
Wall plate stiffness factor	8470 kNm
Total crest acceleration at flexural cracking	2.7 g
Shear deformation	0.141 mm
In-plane flexural deformation	0.0044 mm
1st floor windows shear deformation	0.0006 mm
2nd floor doors shear deformation	0.002 mm
2nd floor windows shear deformation	0.01 mm
Out-of-plane flexural deformation	8.48 mm
In-plane deformation participation	0.025
Out-of-plane deformation participation	0.975
ESDOF generalized mass	7.98 tn
ESDOF generalized stiffness	10398.56 kN/m
ESDOF period	0.17 sec
ESDOF earthquake excitation factor	15.03 tn
ESDOF effective mass ratio	0.35
ESDOF participation factor	1.88

Table 2: Simplified model parameters for URM building (No.1 in Table 1) under transverse/short/weak building plan direction loading. Values are calculated based on Vamvatsikos et al. (2015) [4].

TFM walls are reinforced with timber elements, both horizontal and vertical but also X-type diagonal braces. It is evident historically, since the Bronze Age that the timber reinforcement into masonry walls is strongly related to seismic resistance in earthquake-prone areas. In TFM walls there is also recent experimental and numerical evidence [5] that the contribution of the diagonal braces is vital for walls' lateral behavior in the nonlinear range due to early detachment of the masonry infill from the surrounding timber frame in the event of an earthquake. In addition, it is observed that for very low horizontal displacement the diagonals in tension detach from the surrounding frame. Therefore, it is suggested [5] that the diagonals should contribute to the lateral behavior only in compression and moreover the infill masonry walls of the timber frame should not be considered in the analytical model. Based on these considerations, a macro-model was proposed ([5], [8]) where its input can be easily determined since it involves only the key geometric characteristics of the timber panels and the timber strength. The latter model facilitates the seismic assessment of TFM walls resulting in a valuable tool for simplified seismic vulnerability and risk analyses [9]. Based on the resulting pushover curves produced by pushover analysis [10] of the TFM walls' macro-model, a shape-function is defined for the derivation of the ESDOF properties which is similar to the methodology already described for URM buildings [4]. An example (TFM building No.4 in Table 1) of the resulting pushover curve [10] is given in Fig. 2 and the overall analysis results are tabulated below (Table 3).

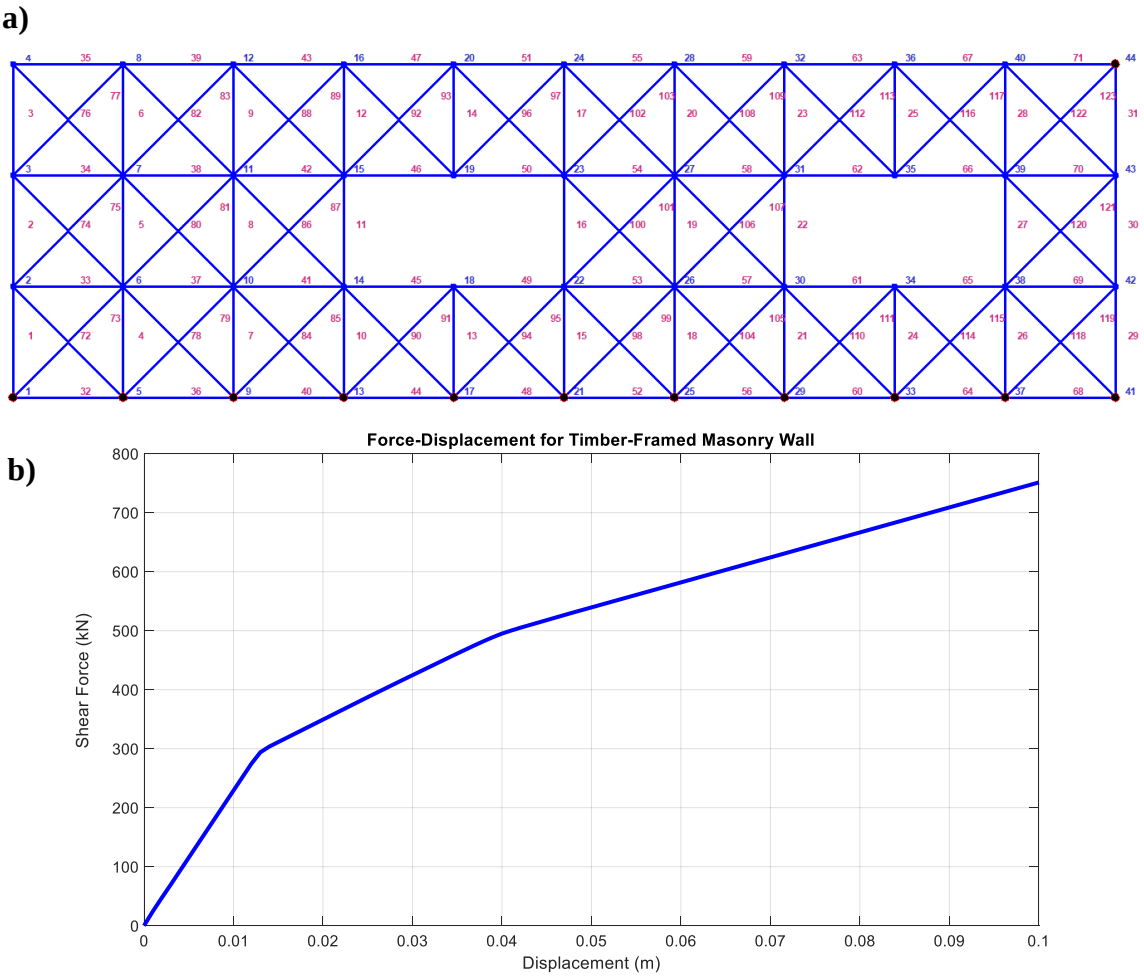

Figure 2: a) TFM wall model with panels incorporating X-type diagonal braces (No.4 in Table 1). b) Pushover curve from the methodology adopted by Kouris et al. (2014) [5].

Longitudinal wall length	7.7 m
Transverse wall length	17 m
Roof height	5.15 m
Wall thickness	0.2 m
Shear Modulus	930 MPa
Shear Strength	0.93 MPa
Wall mass	103.73 tn
Story mass	2.1 tn
Roof mass	3.27 tn
Total mass	109.1 tn
Horizontal "gravity" load	207.83 kN/m
Wall total area	9.88 m^2
Wall box moment of inertia	116.06 m^4
Resistance of wall plan	29.38 m^3
Wall plate stiffness factor	4340 kNm
In-plane deformation (Fig. 2b)	14 mm
Out-of-plane flexural deformation	60.54 mm
In-plane deformation participation	0.188
Out-of-plane deformation participation	0.812
ESDOF generalized mass	15.62 tn
ESDOF generalized stiffness	27653.24 kN/m
ESDOF period	0.15 sec
ESDOF earthquake excitation factor	31.38 tn
ESDOF effective mass ratio	0.58
ESDOF participation factor	2.01

Table 3: Simplified model parameters for TFM building (No.4 in Table 1) under transverse/short/weak building plan direction loading. Values are calculated based on Vamvatsikos et al. (2015) [4].

4 ESTIMATION OF THE NON-STRUCTURAL DAMAGE LEVEL

Considering these real TFM and URM building cases in Alsace France (Table 1) the corresponding fragility curves are derived in terms of peak ground acceleration (PGA) with the aid of structural analysis for a gradually increasing intensity (incremental dynamic analysis - IDA) [11]. The latter analysis of ESDOF of the building cases under study was performed with the MATLAB [12] toolbox FEDEAS Lab [13]. The correlation of the PGA values of the recordings used in the IDA analysis with the corresponding PGV values follows the rule that for very flexible structures (very high fundamental periods) the relative velocity response spectrum of the used record tends to the peak ground velocity (PGV). The induced ground motions obtained from the PEER database were employed and applied in the transverse/short/weak building plan direction ([7], [14]). The fundamental periods of these structures as already mentioned were verified with ambient noise vibration measurements using sensors [5] located at each floor of the buildings under study (Table 1). Moreover, the main geometry required as input for the simplified vulnerability models was taken through field inspection of these buildings. The results are shown in Fig. 3. It can be seen that the fragilities for URM buildings have more or less the same range of probability of damage while the more earthquake resistant TFM building is less fragile for low and medium intensities.

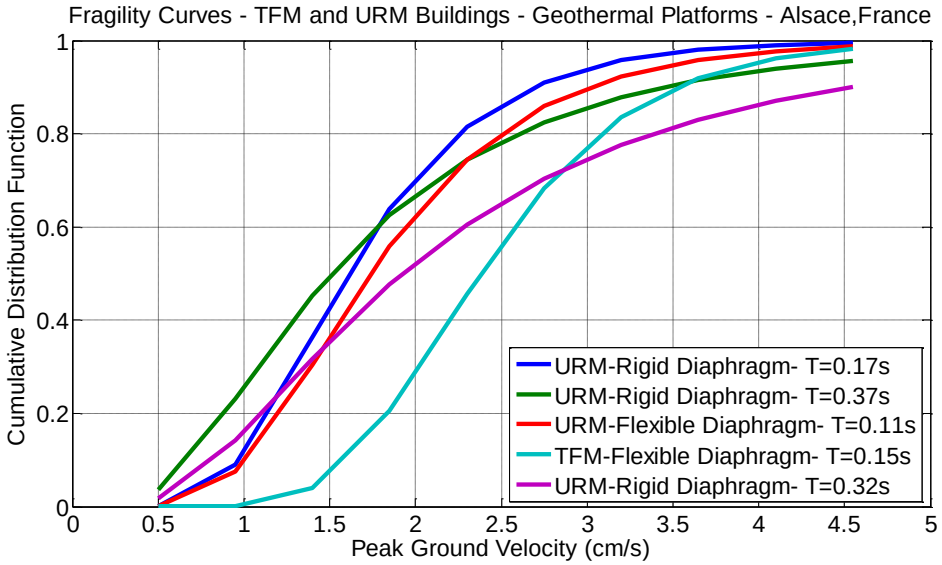

Figure 3: Proposed analytical fragility curves for first damage state (pre-yielding damage state –DS1-0.1% drift limit for non-structural damage) for Unreinforced Masonry Buildings (URM) and Timber-Framed Masonry Buildings (TFM). The buildings are located near the geothermal platforms in Alsace France and are loaded in the weak/short plan view direction of shaking. The fundamental period of these structures was verified with ambient noise measurements through applied sensors [7].

5 CONCLUSIONS

- The estimated dynamic properties for small amplitude vibrations of the historical structures near the geothermal platforms in Alsace, France considered in this work were used to derive simplified vulnerability models.
- Moreover, the Eurocode 8 defines the interstory drift limit of a building for non-structural damage, by looking at its displacement-sensitive non-structural components at the serviceability limit state.
- Therefore, by adopting these limits and the developed simplified vulnerability models, new non-structural fragility curves for typical historical masonry building types dominant in the region under study are proposed.
- The fragility curves have been calculated using incremental dynamic analysis for the seismic demands generally imposed upon linear and slightly non-linear models of single and multiple degrees of freedom, which is the case for the effects of induced seismicity.
- These results will prove useful for both local end-users and industrial stakeholders, with a clear perspective for a better understanding of the risk related to induced and triggered seismicity and its sound management.

REFERENCES

[1] Taghavi, S., Miranda, E. (2003). Response Assessment of Nonstructural Building Elements, *PEER Report 2003/05*, University of California Berkeley.

[2] CEN (2004) *Eurocode 8*: design of structures for earthquake resistance - Part I: general rules, seismic actions and rules for buildings. European Committee for Standardization (CEN). Brussels, Belgium.

[3] Pittore M, Haas M and Megalooikonomou KG (2018) Risk-Oriented, Bottom-Up Modeling of Building Portfolios with Faceted Taxonomies. *Front. Built Environ.* 4:41. doi: 10.3389/fbuil.2018.00041

[4] Vamvatsikos D., Pantazopoulou S. J. (2015) Development of a simplified mechanical model to estimate the seismic vulnerability of heritage unreinforced masonry buildings. *Journal of Earthquake Engineering*, Taylor & Fran, 20(2): 298-325. doi:10.1080/13632469.2015.1060583.

[5] Kouris LAS., Kappos AJ (2014) A practice – oriented model for pushover analysis of a class of timber-framed masonry buildings, *Engineering Structures Journal*, Elsevier, 75: 489-506. doi: 10.1016/j.engstruct.2014.06.012.

[6] Boxberger T, Fleming K, Pittore M, Parolai S, Pilz M, Mikulla S (2017) The Multi-Parameter Wireless Sensing System (MPwise): its description and application to earthquake risk mitigation. *Sensors* 17(10):2400. doi:10.3390/s17102400

[7] Megalooikonomou KG, Parolai S, Pittore M. (2018) Toward performance-driven seismic risk monitoring for geothermal platforms: development of ad hoc fragility curves, *Geothermal Energy*, 6(1):8 , doi: 10.1186/s40517-018-0094-3

[8] Kouris LAS., Kappos AJ (2012) Detailed and simplified non-linear models for timber-framed masonry structures, *Journal of Cultural Heritage*, Elsevier, 13 (1): 47-58. doi: 10.1016/j.culher.2011.05.009.

[9] Kouris L.A.S., Kappos A.J. (2015) Fragility Curves and Loss Estimation for Traditional Timber-Framed Masonry Buildings in Lefkas, Greece. In: Psycharis I., Pantazopoulou S., Papadrakakis M. (eds) Seismic Assessment, Behavior and Retrofit of Heritage Buildings and Monuments. *Computational Methods in Applied Sciences*, vol 37. Springer, Cham. doi: 10.1007/978-3-319-16130-3_8.

[10] Antoniou, S, Pinho, R (2004) Development and verification of a displacement-based adaptive pushover procedure, *Journal of Earthquake Engineering* 8(5), 643–661. doi: 10.1080/13632460409350504.

[11] Vamvatsikos D., Cornell C.A. (2002). Incremental Dynamic Analysis. *Earthquake Engineering and Structural Dynamics*, 31(3): 491-514. doi: 10.1002/eqe.141.

[12] Mathworks. (2017). MATLAB: User's Guide (r2017a).

[13] Filippou F.C., Constantinides M., (2004) FEDEAS Lab – Getting Started Guide and Simulation Examples, *NEESgrid Report 2004-22* and *SEMM Report 2004-05*.

[14] PEER-NGA-East Database (2017). Pacific Earthquake Engineering Research Center, University of California, Berkeley, CA, (http://peer.berkeley.edu/ngaeast/).